Turner et al. Journal of Applied Volcanology (2017) 6:17
DOI 10.1186/s13617-017-0068-3

Journal of Applied Volcanology

RESEARCH Open Access

Lava flow hazard prediction and monitoring with UAS: a case study from the 2014–2015 Pāhoa lava flow crisis, Hawai'i

Nicolas R. Turner[1,2*], Ryan L. Perroy[3] and Ken Hon[4]

Abstract

Accurately predicting lava flow path behavior is critical for active crisis management operations. The advance and emplacement of pāhoehoe flows modifies and inverts pre-existing topography, prompting the need for rapid and accurate updates to the topographic models used to forecast flow paths. The evolution and velocity of pāhoehoe flows are dependent on macro and micro topography, the slope of the descent path, effusion rate, and rheology. During the 2014–2015 Pāhoa crisis on the island of Hawai'i, we used a low-altitude unmanned aerial system (UAS) to quickly and repeatedly image the active front of a slowly advancing pāhoehoe lava flow. This imagery was used to generate a series of 1 m resolution bare-earth digital elevation models (DEMs) and associated paths of steepest descent over the study area. The spatial resolution and timeliness of these UAS-derived models are an improvement over the existing topographic data used by managers during the crisis. Results from a stepwise resampling experiment suggest that the optimum DEM resolution for generating accurate pāhoehoe flow paths through lowland tropical forest environments is between 1 and 3 m. Our updated models show that future flows in this area will likely be deflected by these newly emplaced flows, possibly threatening communities not directly impacted by the original 2014–2015 lava flow. We demonstrate the value of deploying UAS during a dynamic volcanic crisis and suggest that this technology can fill critical monitoring gaps for Kīlauea and other active volcanoes worldwide.

Keywords: Unmanned aircraft system, Pāhoehoe lava flow, Digital elevation model, Hazards, Mapping aid, Crisis response

Background

Pāhoehoe lava flows pose major threats to communities living near active basaltic volcanoes worldwide (Hamilton et al. 2013; Del Negro et al. 2016). Estimating lava flow hazards is important prior to eruptions for regional planning purposes, but becomes critical during times of heightened eruption activity (Gonzalez et al. 2015; Poland et al. 2016; Jenkins et al. 2017). Pāhoehoe lava flows generally move slower than 'a'ā flows; however, they can travel greater distances and spread out over larger areas, posing a more significant long-term threat (Self et al. 1998).

The behavior of an advancing flow is influenced by external and internal factors. External factors include slope gradient, surface roughness, and other topographic and landscape features, while internal factors include variations in lava supply, viscosity, yield strength, rates of inflation, and the geometry of the feeder channels or tube system (Mattox et al. 1993; Kauahikaua et al. 1998; Hon et al. 2003). Over days or weeks, new lobes can break out from the flow front or along margins further upslope, while older lobes can become barriers, deflecting younger flows and altering the original topography (Walker et al. 1991; Hon et al. 1994; Anderson et al. 2012).

Rapid acquisition of high quality topographic data is crucial for monitoring and forecasting lava flow behavior during effusive volcanic crises. Digital Elevation Models (DEMs) are the primary data layer used in models to estimate future lava flow paths and provide flow hazard assessments. The accuracy of the modeled results, either from the paths of steepest descent method (Kauahikaua 2007) or other physics-based lava flow models (e.g., FLOWGO, SCIARA, DOWNFLOW, MAGFLOW),

* Correspondence: nrturner@hawaii.edu
[1]National Disaster Preparedness Training Center, University of Hawai'i at Mānoa, 2500 Campus Rd, Honolulu, HI 96822, USA
[2]Department of Geology and Geophysics, University of Hawai'i at Mānoa, 2500 Campus Rd, Honolulu, HI 96822, USA
Full list of author information is available at the end of the article

depends strongly on how well the DEM represents the physical environment, which can be difficult to determine in heavily vegetated areas (Harris and Rowland 2001; Crisci et al. 2004; Favalli et al. 2005; Negro et al. 2008). As lava flows change the landscape, subsequent flows will travel along new paths of steepest descent, requiring updated DEMs to reflect the dynamic environment. (Kauahikaua 2007; Favalli et al. 2009).

Here we present work done to generate pāhoehoe lava flow paths, based on high resolution topographic models extracted from unmanned aerial system (UAS) imagery collected over the June 27th lava flow during the 2014–2015 eruption event near Pāhoa on the island of Hawai'i. In coordination with Hawai'i County Civil Defense (HCCD) and the U.S. Geological Survey Hawaii Volcano Observatory (HVO), we mapped the pre- and post-flow topography and developed a computational workflow to merge multiple DEMs, filter them of vegetation, and generate projected paths of steepest descent. Future flow paths were also generated to show the impact of the June 27th flow on a potential lava flow in the future that might inundate the area based on the post-flow topography. We compare our UAS-derived results to paths generated from an existing United States Geological Survey (USGS) 10 m DEM used by responding agencies during the 2014–2015 Pāhoa lava flow crisis.

Lava flow monitoring techniques

Active lava flows are monitored and mapped with a variety of techniques, including ground-based surveys and imagery collected by satellites and manned aerial platforms (Poland 2014; Orr et al. 2015; Patrick et al. 2015). Ground-based surveys employing lidar or visible-light imagery with Structure-from-Motion can collect detailed three-dimensional data, but are limited in their spatial coverage and, in the case of lidar, high cost (Cashman et al. 2013; Hamilton et al. 2013). These limitations make ground-based approaches viable for studying isolated features, as opposed to landscape-scale phenomena. Satellites have become essential platforms for remote sensing of active lava flows, providing datasets of large spatial coverage for hazard monitoring (e.g., Higgins et al. 1997; Wright et al. 2008; Harris et al. 2011; Ganci et al. 2012; Patrick et al. 2016). Intermittent cloud cover, coarse spatial image resolution, and long re-acquisition intervals all present problems for these platforms when monitoring dynamic lava flows. Manned helicopters and fixed-wing aircraft provide high-resolution aerial imagery but are expensive to operate, can have difficulties acquiring consistent data, and are normally restricted to higher flight altitudes (above 150 m) for safety reasons.

UAS technology provides several advantages over satellite, manned aircraft, and ground based surveys for data capture over active lava flows. These advantages include (1) low-cost capability for repeat aerial surveys with high temporal resolution; (2) low altitude flight operations for acquiring cm-scale spatial data; (3) automated mission planning and flight operation for consistent datasets; (4) minimal risk to human life in the event of a crash or accident; and (5) the ability to cover an area in high detail without requiring intensive field operations for personnel (Harwin and Lucieer 2012; Westoby et al. 2012; Hugenholtz et al. 2013). For these reasons, small UAS platforms allow frequent data collection over active flows and can be deployed on short notice.

The 2014–2015 Pāhoa lava flow crisis

Hawai'i Island's youngest volcano, Kīlauea volcano is one of the most active volcanoes on earth. In 1983, Kīlauea began an eruption focused at Pu'u 'Ō'ō that continues to erupt at the time of writing (July 2017). Between 1983 and 1991, lava flows from Pu'u 'Ō'ō repeatedly impacted communities in East Hawai'i, burying 184 structures and completely destroying the town of Kalapana. Between 2000 and 2012, an additional 30 homes were destroyed by lava flows to the South-East of Pu'u 'Ō'ō (Kauahikaua et al. 2003; Orr et al. 2013). On June 27th, 2014, a new vent formed on the northeast side of Pu'u 'Ō'ō crater. Pāhoehoe lava from this vent, dubbed the June 27th lava flow, reached the outskirts of the town of Pāhoa in October 2014 and threatened to isolate over 10,000 people in the surrounding area, cutting their ready access to power, water, and critical infrastructure. The June 27th flow continued to threaten communities around Pāhoa until March, 2015, when breakouts ~15 km upslope diverted lava supply away from the front (Poland et al. 2016). The crisis lasted approximately seven months based on disaster declarations, but the June 27th flow was not officially declared inactive until June, 2015.

Methods

UAS flight operations

Our study focused on the lobe of the June 27th flow active from late December, 2014, to March, 2015. We used a small fixed-wing UAS (SenseFly SwingletCAM) with a modified 16.1 megapixel Canon IXUS 127 HS camera to map micro-topography surrounding the active flow front (Fig. 1). UAS flights typically lasted 25 min and the camera payload collected between 100 and 300 geotagged images per flight. We operated under a public certificate of authorization on behalf of the University of Hawaii at Hilo (2014-WSA-60-COA) and under FAA rules that require licensed pilots to keep aircraft within line-of-sight and under 400 ft. (122 m) above ground level (AGL). UAS flights were flown in a grid pattern with 80% frontal and 75% side overlap between image footprints. The camera was triggered autonomously using the onboard flight controller. Each trigger point was pre-determined based

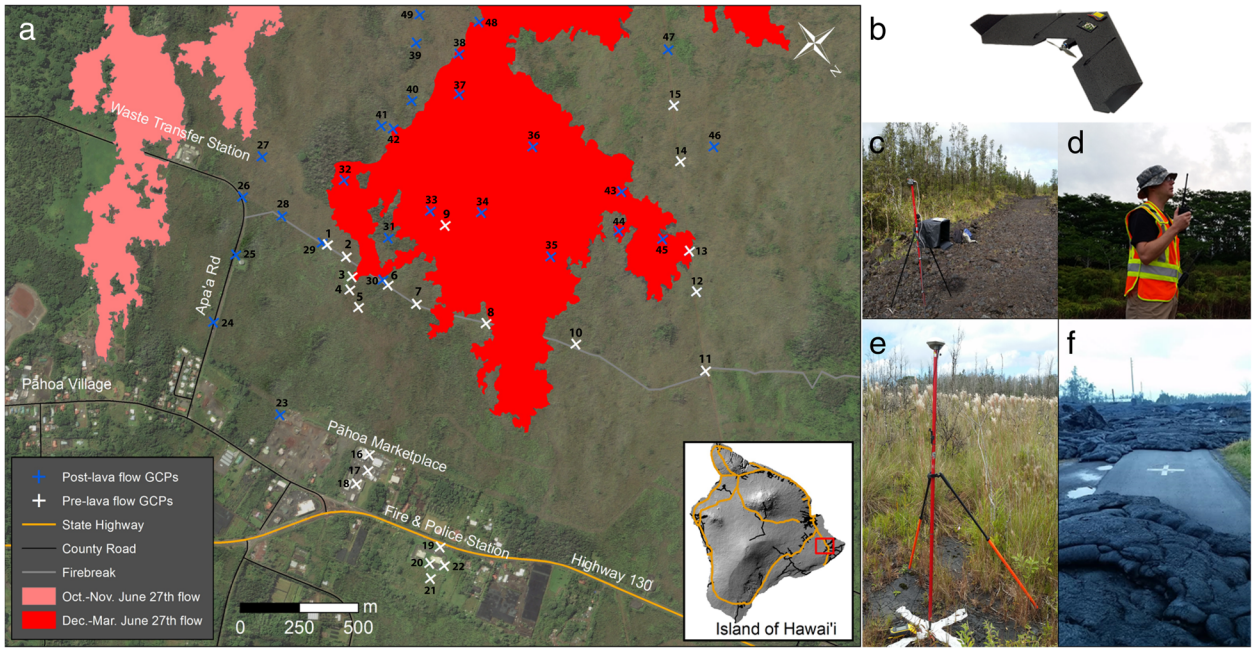

Fig. 1 **a** Map displaying the June 27th flow footprint near the town of Pāhoa. Ground Control Points (GCP) depicted as white crosses (pre-flow GCPs) and blue crosses (post-flow GCPs) with corresponding numbers. In early December, 2014, the County bulldozed a firebreak to contain wildfires sparked by the lava flow. The firebreak provided access to the densely vegetated area for placing GCPs and conducting UAS flights. **b** UAS fixed-wing aircraft used in this study (SenseFly SwingletCAM) **c** Ground control station including laptop, radio telemetry modem, sun-shade box, and tripod. **d** UAS crew member communicating with nearby aircraft using a two-way aviation VHF radio. **e** Obtaining GCP geographic coordinates with a differential GPS Trimble Explorer 6000 unit and Zephyr external antenna. **f** June 27th flow surrounding a GCP

on the uploaded flight plan using eMotion2 flight planning software. Flights were monitored in real-time via visual observers and a radio telemetry (2.4 GHz) link from a laptop computer.

During the Pāhoa crisis, HCCD erected a temporary flight restriction (TFR) around the active flow front, restricting all manned and unmanned aircraft to those directly supporting relief operations. We were granted access to the TFR airspace after receiving permission from both the FAA and Civil Defense with our public Certificate of Authorization and secured ground access from land owners and stakeholders within the study area. During flight operations, we communicated with nearby aircraft using a ground-to-air aviation radio and kept a distance of 1000 ft. (305 m) horizontal and 500 ft. (152 m) vertical to other aircraft. These precautions were important for safely integrating UAS into congested airspace where multiple tour helicopters frequented the outskirts of the flow every hour.

Maintaining direct line of sight with the UAS at all times, as required by FAA regulations, was challenging for operational planning, as the lava flow was surrounded by thick forest with canopy heights >7 m. Flight operations were conducted from new fire-breaks surrounding the perimeter of the flow (Fig. 1) and other clearings. 5581 aerial images were collected from 23 UAS missions between December 14, 2014 and July 26, 2016.

Prior to flights, we placed a series of ground control points (GCP) across the flow field study area to provide positional control and georeference our UAS imagery and derived DEMs (Fig. 1). The three-dimensional coordinates (WGS84, UTM Zone 5 N) for GCP locations were surveyed using a Trimble Geoexplorer 6000 differential GPS with a Zephyr model external antenna mounted on a 2 m pole (Küng et al. 2011; Westoby et al. 2012). Occupation times with the Trimble GPS averaged 10 min and data were post-processed with Trimble Pathfinder Office software using nearby CORS stations. Based on the differential correction report, 71.5% of the corrected positions had an accuracy of 5–15 cm and 99.1% had an accuracy of 30–50 cm or better. Overall, 49 GCPs were deployed across the roughly 5.87 sq. km study area and at least 5 GCPs were included in each UAS flight, distributed across the flight coverage area as evenly as possible. Please refer to Additional file 1: Table S1 for corresponding flights and GCPs used.

To independently assess the accuracy of the UAS derived DEM, an additional 32 points were surveyed across the study area via GPS. These points were collected using the previously described survey technique but

were not included in the UAS image processing steps. Based on the differential correction report for these data, 75.35% of their corrected positions had an accuracy <5 cm and an additional 24.65% had an accuracy between 5 and 15 cm. Absolute elevation values from the GPS survey were then compared to extracted elevation values at the same XY positions for the UAS-derived 1 m DEM and an older 10 m DEM of the Puna district, acquired from the USGS National Elevation Dataset (NED) program and used during the active disaster operations.

Data analysis and processing

An overview of the data processing and analysis workflow is shown in Fig. 2. Imagery and GCP coordinates were processed using structure-from-motion (SfM) software Pix4D Mapper Pro (v2.1.61, Zurich, Switzerland) to generate a high density digital point cloud from each flight. SfM software identifies matching features in an image and extracts three-dimensional points based on multiple geometric views of the same object in the scene by using overlapping photographs (Küng et al. 2011; Westoby et al. 2012). The point clouds from each flight were merged into a single dataset based on the image acquisition date. Flights conducted between Dec 16, 2014 and Jan 18, 2015 were combined and used to generate a 1 m DEM with 0.1 m vertical resolution for pre-flow analysis. Data from UAS flights conducted between Jan 18, 2015 and March 25, 2015, after the completion of the lava flow event, were used to generate a similar DEM for post-flow analysis.

Bare-earth elevation models filtered of vegetation were required for the determination of accurate flow paths. Because passive optical remote sensing techniques rely on reflected light, dense foliage and canopy shadows can conceal the complex topography lying underneath (Dandois et al. 2015; Fraser et al. 2016). In order to generate bare-earth DEMs of the study area, situated within a lowland tropical forest landscape, we needed to filter out surface features such as buildings and vegetation. We employed point cloud filtering techniques using LAStools (rapidlasso GmbH), a lidar software package consisting of a series of powerful batch script algorithms to process point cloud data. The following is a detailed description of the parameters and settings used for each script in LAStools to extract the bare-earth elevation values by filtering the point clouds of vegetation (highlighted

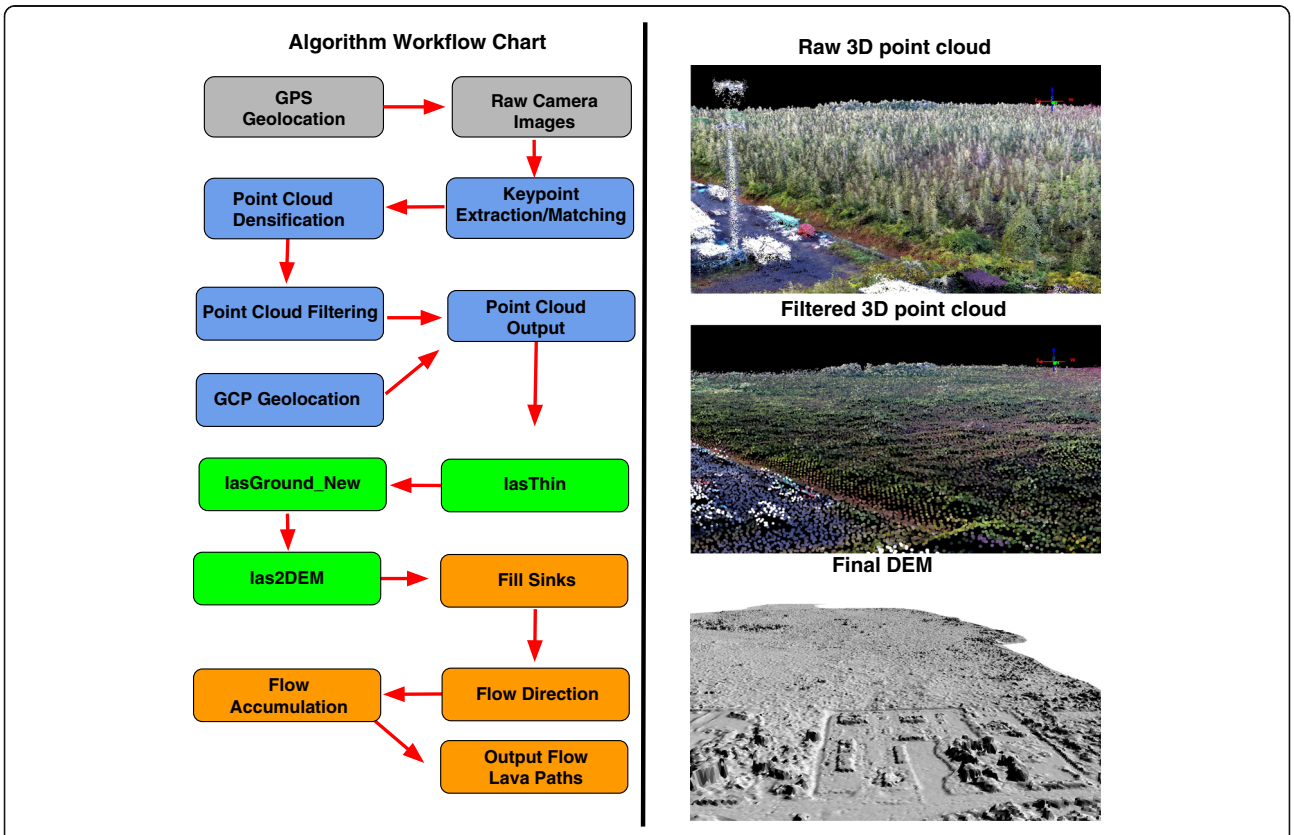

Fig. 2 Left Side: Flow chart summary of the processing workflow beginning with raw aerial images geotagged with onboard GPS (grey); Structure from Motion software processing steps (blue); digital point cloud filtering using LAStools (green); DEM processing to extract paths of steepest descent via ArcGIS hydrology workflow (orange). Right side: (top) raw point cloud before any filtering, (middle) filtered point cloud following removal of vegetation and other structures, (bottom) Hillshade representation of "bare-earth" DEM generated from the filtered point cloud

in green on Fig. 2). Please refer to cs.unc.edu/~isenburg/lastools/ and Isenburg et al. 2006 for additional information. We employed the (1) lasThin tool to thin the point cloud, keeping only the lowest elevation points at a 1 m grid size; (2) lasGround_New tool for bare-earth extraction, classifying the points into ground points (class = 2) and non-ground points (class = 1) using a step size of 1 m (town or flats setting) and an initial search for ground points as '-fine'; and (3) Las2DEM tool to produce a continuous bare-earth digital elevation model (DEM) from the point cloud using the remaining elevation values at a step size of 1 m and exported as a tiff raster format. We chose a 1 m grid size for our pre-flow raster because finer grid sizes detected too much vegetation, which interfered with generating a low-noise DEM from which paths of steepest descent could be generated. Processing time for SfM models typically took several hours on an ASUS computer (CPU: Intel Core i7 3.0 Ghz; 32GB RAM; GPU: NVIDIA Geoforce GTX 970) with additional time required to filter vegetation and run flow path calculations (1–2 additional hours). Pre-lava flow paths were calculated from the DEM generated by UAS overflights in early December, 2014, after an upslope breakout formed a new lobe that ran parallel to the original flow margin and cut off lava supply to the original flow front (Poland et al. 2016; Patrick et al. 2016). Alternative point-cloud processing software or programming libraries (e.g., CloudCompare, QT Modeler, MATLAB, OpenCV) could also be used in place of LAStools.

Tools to calculate paths of steepest descent are common in many Geographic Information System (GIS) software packages, usually falling under hydrology toolsets. For a more detailed discussion on how these paths are calculated please refer to Tarboton et al. 1991; Kauahikaua 2007. The pre-flow DEM was brought into ArcGIS (v10.2) where paths of steepest descent were calculated based on the lavashed concept (Kauahikaua et al. 1995) with the following hydrology workflow: (1) we filled sinks throughout the DEM to ensure proper delineation of stream networks; "sinks" are often errors in the DEM due to rounding of nearest integer values and need to be filled to avoid a discontinuous drainage network; (2) flow direction was calculated using the filled DEM as input in the Spatial Analysis extension and (3) flow accumulation was generated using the flow direction DEM. The final paths of steepest descent were based on the 1 m DEM.

The same workflow was used to produce a filtered 1 m post-lava flow DEM, using imagery collected after the effusive event was over. We also used this same workflow on the USGS 10 m DEM (Fig. 3, blue lines). The 10 m bare-earth USGS DEM was the highest-resolution elevation dataset publicly available at the time of the event and was derived from USGS 7.5′ minute DEM Quads produced by NED (1983). USGS and Civil Defense utilized helicopter and ground surveys to produce a series of maps depicting the flow's outline and evolution during the crisis. We compared our projected paths of steepest descent to the lava flow's actual progression using a time-series of flow outline GIS polygons provided by USGS and Civil Defense.

We also examined the impact of DEM spatial resolution on lava flow paths. This was done by resampling our UAS-derived DEM at progressively coarser resolutions, up to 10 m resolution in 1 m increments, and calculating the resulting paths of steepest descent at each step using a comparable flow accumulation threshold (Jenson and Domingue 1988).

Like hydrologic watershed boundaries for stream networks, the contributing areas of potential lava flow paths can be delineated based on topography. Lavasheds represent the area in which a given flow path can be identified and serve as a way to identify possible paths of steepest descent at varying resolutions (Kauahikaua et al. 1995). Calculating these lavasheds can provide a more synoptic view of the potential paths a flow may travel within a confined geographic area. Lavasheds were calculated using the ArcGIS watershed geoprocessing tool, and pour points were set at every fork between paths of steepest descent producing a lavashed per path. To quantify the ratio of flow length and total area of a unit watershed, the length of each flow path per lavashed unit was divided by the total area of that given lavashed unit. The mean of all lavasheds and flow lengths were taken for each DEM. The flow path length / lavashed area was then converted to a logarithmic scale with a base of 10.

Results

A key component of this study was to determine how well the UAS-derived DEMs performed in terms of characterizing the landscape and supporting lava hazard predictions. Paths of steepest descent were generated from our UAS-derived 1 m bare-earth DEM (pre-flow) and the USGS 10 m DEM used during the active disaster operations and overlain against the time-series of flow field outlines mapped by Hawaii Volcano Observatory (Fig. 3). The elevational accuracy of the two DEMs, as measured against a differential GPS survey of 32 independent points distributed around the study area, was determined and found to be quite similar, with an RMSE value of 0.69 for the 1 m DEM and 0.74 for the 10 m DEM (Fig. 4).

Results from the resampling experiment to determine the effect of DEM spatial resolution on paths of steepest descent and lavashed delineation are shown in Fig. 5. Individual lavasheds are outlined in black within the larger orange polygons, with lines of steepest descent depicted as yellow lines. As the number of possible lavasheds decreases with coarsening spatial resolution, the flow path

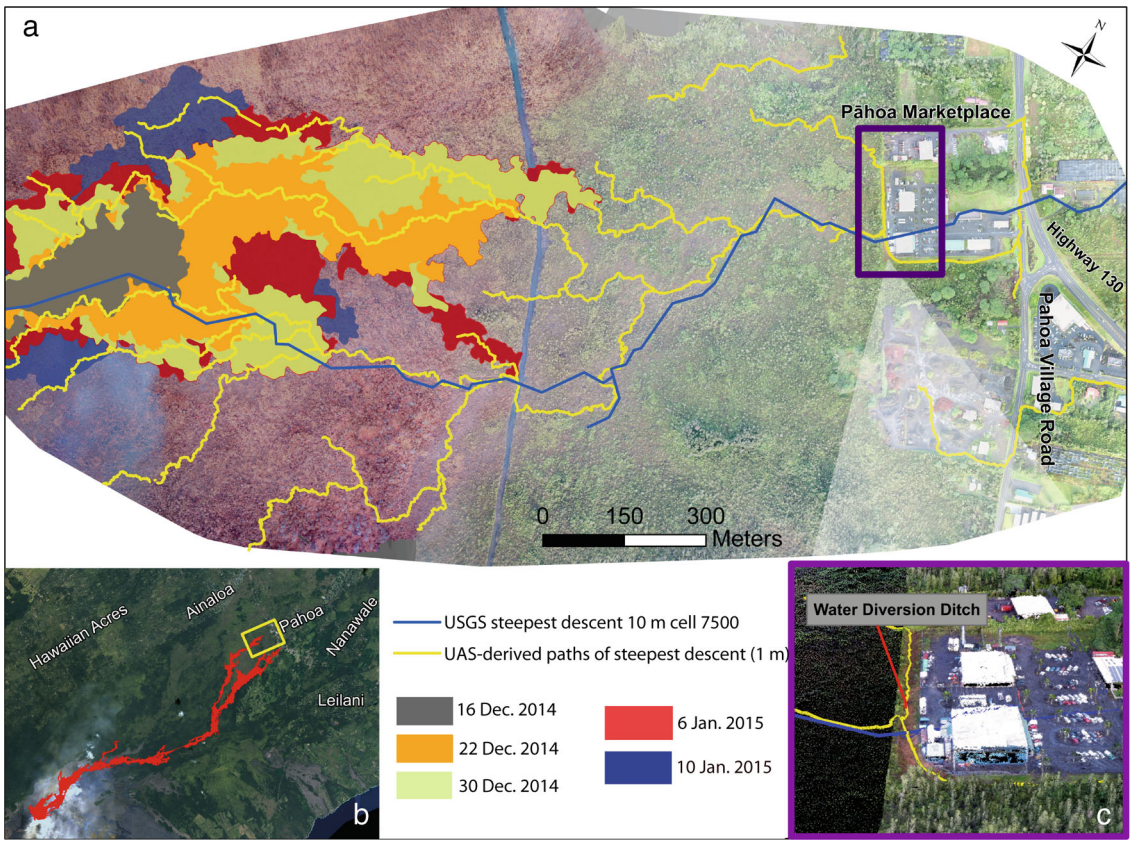

Fig. 3 a Comparison between 1 m UAS-derived flow paths (yellow lines) and 10 m USGS DEM (blue lines). The advancing lava flow is depicted as a series of flow outlines produced from HVO field mapping from Dec 16, 2014 through Jan 10, 2015. The 1 m UAS flow paths were generated from data collected on Dec 16, 2014 – Dec 17, 2014. The purple box highlights the area of panel c. Refer to USGS, 2017 to search for June 27th flow maps. **b** Final extent of the June 27th lava flow. **c** UAS-derived 3D point cloud showing the 5 m ditch surrounding the Pāhoa marketplace, a topographic feature that was not identified from the 10 m USGS DEM due to coarse spatial resolution

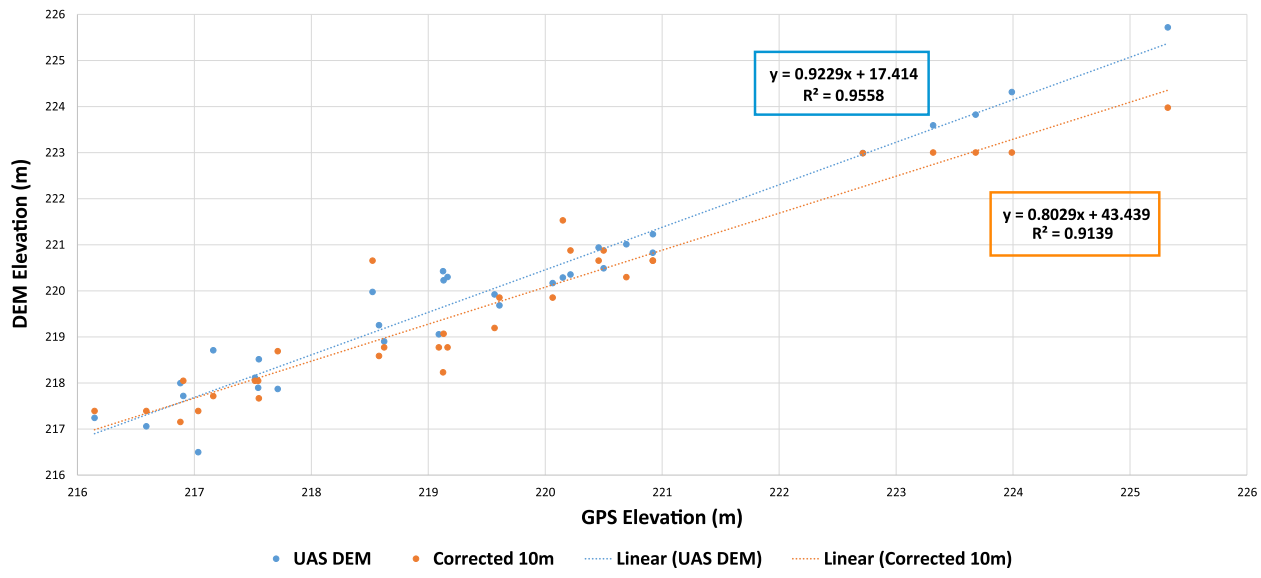

Fig. 4 Elevation values from an independent GPS survey of 32 points collected within the area of the pre-flow DEM plotted against elevation values extracted from the 1 m UAS-derived DEM (blue dots) and the 10 m USGS DEM (orange dots)

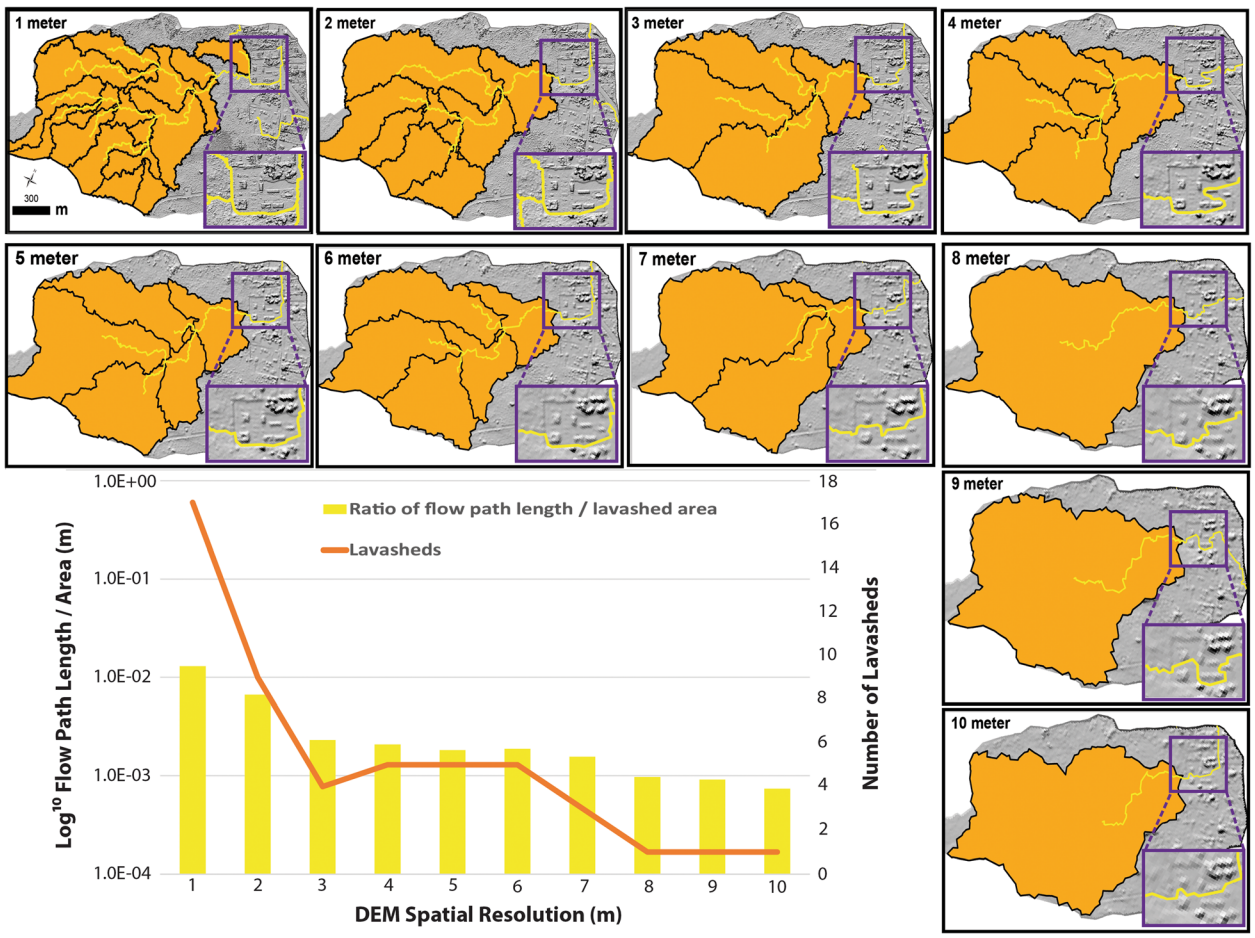

Fig. 5 Series of resampled UAS-derived DEMs showing the loss of detail with coarser resolution data depicted in the varying lavasheds (orange) and the total length of flow paths in a given lavashed. Within each lavashed inset is a blow-up of the 5 m ditch surrounding the Pāhoa Marketplace. The 5 m ditch was excavated during construction of the Pāhoa Marketplace in 2004. Graph showing the step-wise series of DEMs decreasing in spatial resolution from 1 m to 10 m, the effect on total lavasheds per DEM and the ratio of flow length path / lavashed area

length for each path of steepest descent within a given lavashed unit decreases as well (Fig. 5).

Discussion

Implications for lava flow monitoring

The short-term behavior of long-lived pāhoehoe flows is difficult to predict, as advancing lava is influenced by new breakouts at the front or along the margins of an active flow and requires a continuous supply of new lava through the molten core (Kauahikaua et al. 1998; Hamilton et al. 2013). During the Pāhoa lava flow crisis, early forecasts of flow behavior were thwarted by hidden ground cracks in the Puna forest reserve (Poland et al. 2016). Accurate and up-to-date measurements of underlying topography are crucial for flow behavior analysis, and are a critical gap in eruption monitoring that UAS can fill.

An example of this can be seen around the Pāhoa Marketplace, built in 2004, where the NED 10 m DEM flow paths pass directly over a 5 m wide water diversion ditch surrounding the development (Fig. 3). The primary reason this occurs is because the 10 m DEM was generated prior to the construction of the Pāhoa Marketplace and excavation of the drainage ditch. A second reason is due to the coarseness of the 10 m DEM. Based on our resampled DEM experiment (Fig. 5) we see that DEMs with a resolution >6 m do not pick up this feature, while UAS-derived DEMs with a resolution below 5 m produced flow paths that recognized the water diversion ditch. While it is unclear how or if the ditch would influence final emplacement of the flow, it is a substantial topographic feature that coarser datasets, even up-to-date ones, do not detect. Higher spatial resolution DEMs allow for a higher number of lavasheds to be detected (Fig. 5), making them valuable for short-term hazard assessments.

Fortunately, the June 27th lava flow stopped short of overrunning Pāhoa and stagnated by March, 2015,

eliminating the threat to nearby communities. However, scientists and emergency planners concerned with future lava flows can benefit from long-term hazard planning using UAS datasets. Post-flow modeling using UAS-derived data shows the influence of the 2014–2015 flows on diverting the paths of future lava flows into completely new directions (Fig. 6), making lava flow hazard studies based on the pre-flow obsolete. To help improve response efforts for future lava flows, acquiring more recent and higher resolution DEMs would benefit any region previously inundated by lava flows.

Additional insight on the future behavior of a flow could be gleaned by finding the critical threshold at which a pāhoehoe flow will jump between given lavasheds (Fig. 5) based on flow parameters such as size, mass flux, and surrounding topography. How important the boundaries of a given lavashed are in constraining the direction of a flow will depend greatly on the current stage of maturity in an ongoing eruption, the type of flow (e.g., sheet flow, hummocky tube-fed flow), current topography, and the context of the response efforts (short-term or long-term hazard planning). High resolution DEMs can provide important information towards observing the boundary at which flow paths diverge (Hon et al. 1994; Hamilton et al. 2013).

Lava flow monitoring with UAS can provide high spatial resolution DEMs with the capability for frequent and cost-effective overflights to reflect new changes

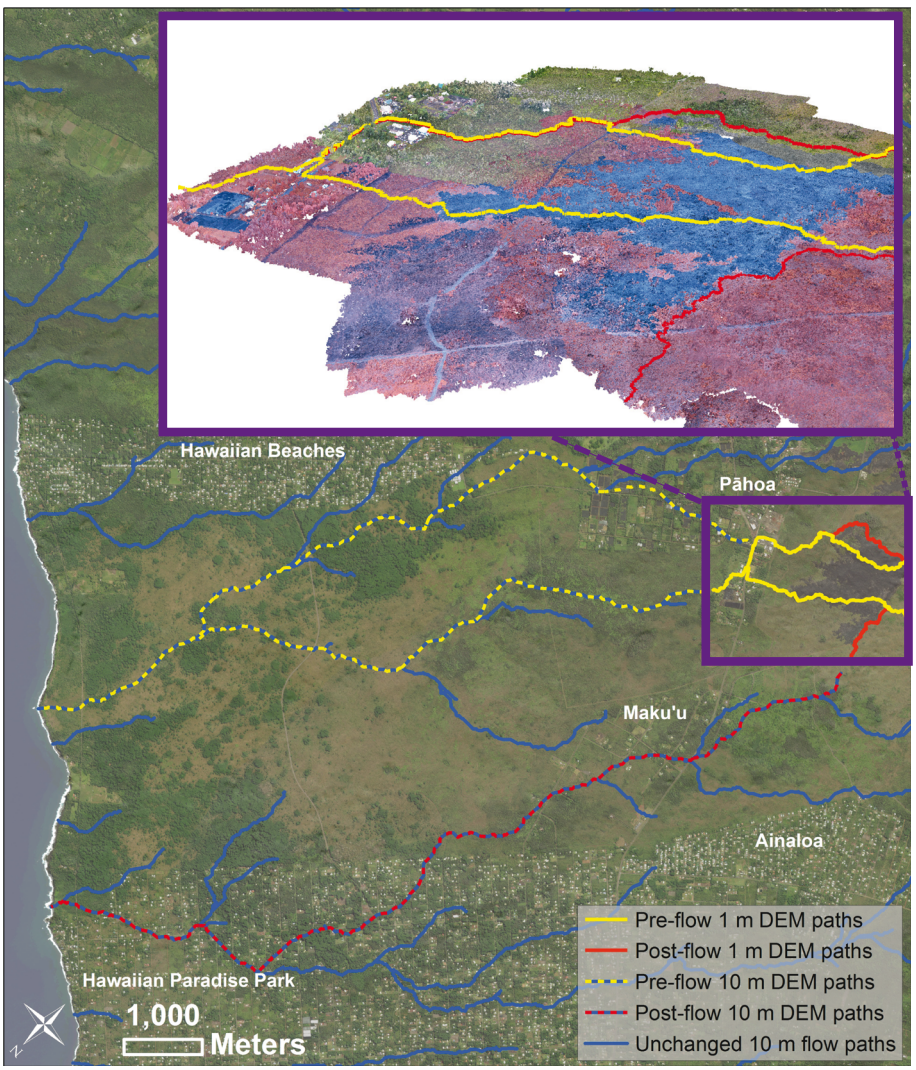

Fig. 6 Comparison of the pre-lava flow paths the June 27th flow would have followed (pre-flow solid yellow lines based on UAS 1 m DEM, pre-flow dashed yellow and blue lines based on 10 m DEM) to the new paths future flows will follow (post-flow solid red lines based on UAS 1 m DEM, post-flow dashed red and blue lines based on 10 m DEM). Purple box delineates boundary of 1 m DEM; outside of this the unchanged USGS 10 m flow paths are shown in blue. Puna communities are labelled by region. The deflection of new flows (zoomed inset panel in purple) now poses a greater hazard to the communities of Maku'u and Hawaiian Paradise Park

caused by flow activity. The datasets provide a detailed record of morphological changes across the flow field, serving as a time-series digital repository of observations on pāhoehoe behavior. This can be of high importance during a prolonged effusive crisis because eruptions can span weeks to years, and budget limitations control the frequency of helicopter overflights to monitor lava flows (Patrick et al. 2016; Orr et al. 2015b). A key observation from a HVO study on the 2014–2015 flow showed a large percentage of surface activity occurring away from the immediate flow front in the form of lateral breakouts well behind the active front (Patrick et al. 2016), underscoring the importance of extending the operational range of UAS to capture areas beyond the active front of an advancing pāhoehoe flow. Doing so would extend the benefits of higher spatial and temporal resolution across the entire flow and throughout the flow's evolution.

Applications for other lava flow models

This work has focused on the lines of steepest descent technique, one of the simplest methods for predicting lava flow paths (Kauahikaua 2007). However, more sophisticated lava flow modelling efforts, including stochastic slope-controlled models (Harris and Rowland 2001; Favalli et al. 2005), cellular automata models (Crisci et al. 2004; Del Negro et al. 2005; Vicari et al. 2007), and other numerical simulations (Dietterich et al. 2015), also rely on high quality DEMs input layers to produce successful results. UAS provide a means of effectively generating these needed DEMs, regardless of the modeling method. For models that are computationally complex, simulation run time is an important factor to consider for the results to be of value, especially during an active crisis that demands quick and frequent updates to changing conditions. The ability of UAS to rapidly and continuously update changes in topography can reduce or even negate the requirement for running multiple flow paths in a stochastic simulation. Beyond collecting the UAS data, an important aspect of effectively incorporating this technology into hazard operations will come from automating the DEM post-processing steps (e.g., vegetation filtering, combining multiple flights) as much as possible to make new DEMs more readily accessible for given scenarios.

Successful volcano monitoring with UAS

The successful integration of UAS into active volcano monitoring programs still has challenges, including evolving aviation regulations. In the United States, the Federal Aviation Administration has released its small UAS regulation Part 107, which permits UAS flights by pilots that pass a remote pilot exam. Waivers can be acquired to do special types of flying such as night operations, flying beyond line-of-sight (BLOS), and having a single UAS pilot control multiple aircraft simultaneously commonly referred to as SWARM flights (Diaz et al. 2015). For most eruption settings, large-scale monitoring over the length of the entire flow field will require BLOS flying and/or the use of SWARM technology with multiple UAS mapping sections of the lava flow simultaneously. In the future, these types of operations can significantly enhance the monitoring capability of volcano observatories worldwide within existing monitoring programs. In addition, UAS-derived topographic datasets can be easily combined with other monitoring tools such as thermal infrared mapping and field-based measurements of pāhoehoe flow inflation and advancement (Patrick et al. 2016). The increased mapping frequency UAS flights afford, due to their low operational costs, can be a substantial boost to effective monitoring and tracking of both pāhoehoe and a'ā lava flows at effusive volcanoes worldwide.

During response efforts for the Pāhoa crisis, all imagery and related data products from this project (DEM, orthomosaics) were shared with both emergency managers at Civil Defense and scientists at HVO. Although UAS data were shared as quickly as possible, final delivery of data products often took 1–2 days due to field logistics, travel time, computational processing, and coordinating with Civil Defense analysts. If UAS are to be used effectively in a future crisis, increased data workflow automation can prevent staleness of information. Other advancements in UAS technology, including connecting field operations to the internet via cloud related hardware, can allow field teams to share imagery in near-real time. Structure-from-Motion processing could be done in the cloud or imagery downloaded locally to be processed before teams even leave the field. Other approaches include computer vision based machine learning models to extract only the most relevant information from UAS imagery (e.g., classifying and extracting fresh lava), reducing bandwidth requirements and transferring only the most critical data during flight. If placement of GCPs are too dangerous for UAS crews, other technologies such as high precision real time kinematic (RTK) GPS or omitting GCPs entirely and sacrificing DEM accuracy are possible alternative approaches. The most successful future integration of UAS for volcano monitoring programs will likely include all of the above as observatories supplement existing monitoring networks (e.g., seismic networks, GPS stations, gas monitoring, weather stations) with UAS technology.

Additional applications for UAS in lava flow monitoring

Beyond continuous updates to changes in topography and generating high resolution DEMs, products derived from this work can be used to gain additional insights into the emplacement processes of active pāhoehoe flows, including detailed measurements of lava flow inflation rates,

flow thickness, volumetric flow rates, and characterization of features (e.g., tumulus formation, surface vs lateral breakouts, sinuous inflation ridges, hummocky vs sheet morphology, lava partitioning) over spatially and temporally useful scales to improve emergency response efforts (Perroy et al., 2015). Consecutive Structure-from-Motion derived three-dimensional surface models of the flow, collected over hours to weeks, can effectively track the advancement of a flow, formation of a master tube system, and related breakouts. Merging these datasets with aerial thermal infrared imagery captured contemporaneously may yield new insights into flow emplacement behavior (Patrick et al. 2016).

UAS technology can provide a detailed synoptic view of a flow's evolution and emplacement behavior, possibly spurring the development of new predictive models designed specifically for pāhoehoe lava flows. These models will need to incorporate the complexity of an actively evolving flow field including the development of a master tube system prone to leakage, identify the morphology of breakouts (e.g., sheet and hummocky lava), reflect changes in lava supply/storage through inflation rates, and rapidly update the modifications in topography. UAS provide the capability to collect this type of data both spatially and temporally.

Conclusions

We demonstrate a new approach to generate updated pāhoehoe lava flow paths, based on high resolution topographic models extracted from unmanned aerial system (UAS) imagery during the 2014–2015 Pāhoa lava flow crisis. UAS provide a means of rapidly assessing changing field conditions and reducing the uncertainty in lava flow behavior based on topographic constraints. This ability can make a significant difference for hazard mitigation efforts by calculating new paths of steepest descent immediately following alteration of the physical environment. The repeat collection of digital x-y-z point cloud data can be used for long-term monitoring and analysis of lava flow evolution. The potential benefits of UAS in repeated deployments over active lava flows include:

(1) Generate high spatial resolution DEMs from low-altitude UAS flights using low-cost optical sensors.
(2) Better estimate future flow path behavior and reduce uncertainty in hazard forecasts.
(3) Improve the frequency and quality of data collected by volcano monitoring programs, due to the low operational costs of UAS and their ability to fly on short notice.
(4) Capture new topographic changes caused by pāhoehoe flow inflation, providing detailed updates to obsolete topographic datasets that were not possible before.
(5) Supplement existing remote sensing (e.g., satellite and manned aircraft) and field based monitoring of active flows.

As UAS technology progresses and matures, we believe future monitoring efforts that utilize UAS will fill a critical gap in volcano monitoring. UAS hold great potential for improving response efforts during a volcanic crisis and are an effective tool for mapping changes for both short-term and long-term lava flow hazard assessments.

Additional file

Additional file 1: Table S1. For each UAS flight the corresponding GCPs are listed that were used in processing with SfM software. Additional columns include Date of flight, number of photos captured, and the number of GCPs used in SfM processing for that flight. (PDF 45 kb)

Acknowledgements

We would like to acknowledge the hard work of Nathan Stephenson and Arthur Cunningham for their help in the field with UAS operations; Victor Rasgado for his time and equipment as well as help from his students at Hawaii Community College; Donald Straney for his support with equipment and personnel funding; Daryl Oliveria and the dedicated staff at Hawaii County Civil Defense for their support, access to field sites, and close coordination during the crisis; and Tim Orr, Matthew Patrick, and the staff of Hawaii Volcano Observatory for their professionalism and field support. Parrot senseFly provided a second SwingletCAM aircraft during the crisis; their support was greatly appreciated. Suggestions from Jan Lindsay and two anonymous reviewers greatly improved the final manuscript and NRT would also like to thank Bruce Houghton and Sebastien Biass for their helpful comments.

Authors' contributions

All authors have reviewed this manuscript and contributed to its content. All authors read and approved the final manuscript.

Funding

NRT is grateful for support from the University of Hawaii at Hilo Office of the Chancellor during the crisis and from the National Disaster Preparedness Training center during the writing of this manuscript. This material is based upon work supported by the National Science Foundation Graduate Research Fellowship under Grant No. (1329626). This work was partially funded by NASA EPSCoR Grant NNX15ANZZA.

Competing interests

The authors declare that they have no competing interests.

Publisher's Note

Author details

[1]National Disaster Preparedness Training Center, University of Hawai'i at Mānoa, 2500 Campus Rd, Honolulu, HI 96822, USA. [2]Department of Geology and Geophysics, University of Hawai'i at Mānoa, 2500 Campus Rd, Honolulu, HI 96822, USA. [3]Department of Geography and Environmental Science, University of Hawai'i at Hilo, 200 W Kawili St, Hilo, HI 96720, USA. [4]Department of Geology, University of Hawai'i at Hilo, 200 W Kawili St, Hilo, HI 96720, USA.

Received: 2 May 2017 Accepted: 20 October 2017
Published online: 02 November 2017

References

Anderson SW, Smrekar SE, Stofan ER. Tumulus development on lava flows: insights from observations of active tumuli and analysis of formation models. Bull Volcanol. 2012;74:931–46. doi:10.1007/s00445-012-0576-2.

Cashman KV, Soule SA, Mackey BH, et al. How lava flows: new insights from applications of lidar technologies to lava flow studies. Geosphere. 2013;9:1664–80. doi:10.1130/GES00706.1.

Crisci GM, Rongo R, Di Gregorio S, Spataro W. The simulation model SCIARA: the 1991 and 2001 lava flows at Mount Etna. J Volcanol Geotherm Res. 2004;132:253–67. doi:10.1016/S0377-0273(03)00349-4.

Dandois JP, Olano M, Ellis EC. Optimal altitude, overlap, and weather conditions for computer vision uav estimates of forest structure. Remote Sens. 2015;7:13895–920. doi:10.3390/rs71013895.

Del Negro C, Fortuna L, Vicari A (2005) Modelling lava flows by Cellular Nonlinear Networks (CNN): preliminary results. Nonlinear Process Geophys v. 12:505–513–7946-12–505. doi:10.5194/npg-12-505-2005

Diaz JA, Pieri D, Wright K, et al. Unmanned aerial mass spectrometer Systems for in-Situ Volcanic Plume Analysis. J Am Soc Mass Spectrom. 2015;26(2):292–304. doi:10.1007/s13361-014-1058-x.

Dietterich H, Lev E, Chen J, et al (2015) Benchmarking computational fluid dynamics models for application to lava flow simulations and hazard assessment [abs.]. Am Geophys Union, Fall Meet 2015 Abstr abstract no. V13D–07. doi:10.1186/s13617-017-0061-x

Favalli M, Mazzarini F, Pareschi MT, Boschi E. Topographie control on lava flow paths at Mount Etna. Italy: Implications for hazard assessment J Geophys Res Earth Surf. 2009; doi:10.1029/2007JF000918.

Favalli M, Pareschi MT, Neri A, Isola I. Forecasting lava flow paths by a stochastic approach. Geophys Res Lett. 2005;32:1–4. doi:10.1029/2004GL021718.

Fraser RH, Olthof I, Lantz TC, Schmitt C. UAV photogrammetry for mapping vegetation in the low-Arctic. Arct Sci. 2016;102:1–51. doi:10.1139/as-2016-0008.

Ganci G, Harris AJL, Del Negro C, et al. A year of lava fountaining at Etna: volumes from SEVIRI. Geophys Res Lett. 2012;39:1–6. doi:10.1029/2012GL051026.

Gonzalez PJ, Bagnardi M, Hooper AJ, et al. The 2014-2015 eruption of Fogo volcano: geodetic modeling of Sentinel-1 TOPS interferometry. Geophys Res Lett. 2015;42:9239–46. doi:10.1002/2015GL066003.

Hamilton CW, Glaze LS, James MR, Baloga SM. Topographic and stochastic influences on pāhoehoe lava lobe emplacement. Bull Volcanol. 2013;75:1–16. doi:10.1007/s00445-013-0756-8.

Harris AJL, Favalli M, Wright R, Garbeil H. Hazard assessment at Mount Etna using a hybrid lava flow inundation model and satellite-based land classification. Nat Hazards. 2011;58:1001–27. doi:10.1007/s11069-010-9709-0.

Harris AJL, Rowland SK. FLOWGO: a kinematic thermo-rheological model for lava flowing in a channel. Bull Volcanol. 2001;63:20–44. doi:10.1007/s004450000120.

Harwin S, Lucieer A. Assessing the accuracy of georeferenced point clouds produced via multi-view stereopsis from unmanned aerial vehicle (UAV) imagery. Remote Sens. 2012;4:1573–99. doi:10.3390/rs4061573.

Hon K, Gansecki C, Kauahikaua J. The transition from "a"ā to pāhoehoe crust on flows emplaced during the Pu'u "Ō"ō-Kūpaianaha eruption. USGS Prof Pap. 2003;1676:89–103.

Hon K, Kauahikaua J, Denlinger R, Mackay K. Emplacement and inflation of pahoehoe sheet flows: observations and measurements of active lava flows on Kilauea volcano, Hawaii. Geol Soc Am Bull. 1994;106:351–70. doi:10.1130/0016-7606(1994)106<0351:EAIOPS>2.3.CO;2.

Hugenholtz CH, Whitehead K, Brown OW, et al. Geomorphological mapping with a small unmanned aircraft system (sUAS): feature detection and accuracy assessment of a photogrammetrically-derived digital terrain model. Geomorphology. 2013;194:16–24. doi:10.1016/j.geomorph.2013.03.023.

Isenburg M, Liu Y, Shewchuk J, et al. Generating raster DEM from mass points via TIN streaming. GIScience'06 Conf Proc. 2006;4197:186–98. doi:10.1007/11863939_13.

Jenkins SF, Day SJ, Faria BVE, Fonseca JFBD. Damage from lava flows: insights from the 2014–2015 eruption of Fogo, Cape Verde. J Appl Volcanol. 2017;6:6. doi:10.1186/s13617-017-0057-6.

Jenson SK, Domingue JO. Extracting topographic structure from digital elevation data for geographic information system analysis. Photogramm Eng Remote Sensing. 1988;54:1593–600.

Kauahikaua J. Lava flow hazard assessment, as of August 2007, for Kilauea east rift zone eruptions, Hawaii island. US Geol Surv Open-File Rep. 2007;9:2007–1264.

Kauahikaua J, Cashman KV, Mattox TN, et al. Observations on basaltic lava streams in tubes from Kilauea volcano, island of Hawai'i. J Geophys Res Solid Earth. 1998;103:27303–23. doi:10.1029/97JB03576.

Kauahikaua JP, Margriter SC, Lockwood JP, Trusdell FA. Applications of GIS to the estimation of lava flow hazards on Mauna Loa Volcano, Hawai'i. In: Rhodes JM, Lockwood JP, editors. Mauna Loa revealed; structure, composition, history, and hazards: American Geophysical Union Geophysical Monograph 92; 1995. p. 315–25.

Kauahikaua JP, Sherrod DR, Cashman KV, et al. Hawaiian lava-flow dynamics during the Pu'u "O"o-Kupaianaha eruption: a tale of two decades. US Geol Surv Prof Pap. 2003;1676:63–87.

Küng O, Strecha C, Beyeler A, et al. The accuracy of automatic photogrammetric techniques on ultra-light UAV imagery. ISPRS - Int arch Photogramm remote Sens spat. Inf Sci. 2011;XXXVIII-1/:125–30. doi:10.5194/isprsarchives-XXXVIII-1-C22-125-2011.

Mattox TN, Heliker C, Kauahikaua J, Hon K. Development of the 1990 Kalapana flow field, Kilauea volcano, Hawaii. Bull Volcanol. 1993;55:407–13. doi:10.1007/BF00302000.

Del Negro C, Cappello A, Ganci G (2016) Quantifying lava flow hazards in response to effusive eruption. Bull Geol Soc Am 128:1–13. doi:10.1130/B31364.1.

Negro C, Fortuna L, Herault A, Vicari A. Simulations of the 2004 lava flow at Etna volcano using the magflow cellular automata model. Bull Volcanol. 2008;70:805–12. doi:10.1007/s00445-007-0168-8.

Orr TR, Bleacher JE, Patrick MR, Wooten KM. A sinuous tumulus over an active lava tube at Kīlauea volcano: evolution, analogs, and hazard forecasts. J Volcanol Geotherm Res. 2015;291:35–48. doi:10.1016/j.jvolgeores.2014.12.002.

Orr TR, Heliker C, Patrick MR. The ongoing Pu'u 'O'o eruption of Kllauea Volcano, Hawai'i—30 years of eruptive activity. US Geol Surv Fact Sheet. 2013;6:2012–3127.

Patrick M, Orr T, Fisher G, et al. Thermal mapping of a pāhoehoe lava flow. Kīlauea Volcano J Volcanol Geotherm Res. 2016; doi:10.1016/j.jvolgeores.2016.12.007.

Patrick MR, Kauahikaua J, Orr T, et al (2015) Operational thermal remote sensing and lava flow monitoring at the Hawaiian Volcano Observatory. Geol Soc London, Spec Publ SP426.17-. doi:10.1144/SP426.17

Perroy RL, Turner NR, Ken Hon VR. Monitoring inflation and emplacement during the 2014–2015 Kilauea lava flow with an unmanned aerial vehicle. In: American Geophysical Union; 2015. p. 1.

Poland MP. Time-averaged discharge rate of subaerial lava at Kīlauea volcano, Hawai'i, measured from TanDEM-X interferometry: implications for magma supply and storage during 2011–2013. Jounral of geophysical research. 2014;119:5464–81.

Poland MP, Orr TR, Kauahikaua JP, et al. The 2014-2015 Pāhoa lava flow crisis at Kīlauea volcano, Hawai'i: disaster avoided and lessons learned. GSA TODAY | FEBRUARY 2016 GSA TODAY. 2016;26:4–10. http://www.geosociety.org/gsatoday/archive/26/2/article/i1052-5173-26-2-4.htm. doi:10.1130/GSATG262A.1.4.

Self S, Keszthelyi L, Thordarson T. The importance of Pāhoehoe. Annu Rev Earth Planet Sci. 1998;26:81–110. https://doi.org/10.1146/annurev.earth.26.1.81.

Tarboton D, Bras R, Rodriguez-Iturbe I. On the extraction of channel networks from digital elevation data. Hydrol Process. 1991;5:81–100. doi:10.1002/hyp.3360050107.

Vicari A, Alexis H, Del Negro C, et al. Modeling of the 2001 lava flow at Etna volcano by a cellular automata approach. Environ Model Softw. 2007;22:1465–71. doi:10.1016/j.envsoft.2006.10.005.

Westoby MJ, Brasington J, Glasser NF, et al. "Structure- from- motion" photogrammetry: a low- cost, effective tool for geoscience applications. Geomorphology. 2012;179:300–14. doi:10.1016/j.geomorph.2012.08.021.

Wright R, Garbeil H, Harris AJL. Using infrared satellite data to drive a thermo-rheological/stochastic lava flow emplacement model: a method for near-real-time volcanic hazard assessment. Geophys Res Lett. 2008;35:1–5. doi:10.1029/2008GL035228.